Multi-objective optimization of laminated composite beam structures using NSGA-II algorithm

Vo-Duy, T.; Duong-Gia, D.; Ho-Huu, V.; Vu-Do, H. C.; Nguyen-Thoi, T.

DOI
10.1016/j.compstruct.2017.02.038

Publication date
2017

Document Version
Accepted author manuscript

Published in
Composite Structures

Citation (APA)
Vo-Duy, T., Duong-Gia, D., Ho-Huu, V., Vu-Do, H. C., & Nguyen-Thoi, T. (2017). Multi-objective optimization of laminated composite beam structures using NSGA-II algorithm. *Composite Structures*, *168*, 498-509. https://doi.org/10.1016/j.compstruct.2017.02.038

Post print in : Composite Structures
Volume 168, 15 May 2017, Pages 498–509
Link to formal publication (Elsevier): http://dx.doi.org/10.1016/j.compstruct.2017.02.038

Multi-objective optimization of laminated composite beam structures using NSGA-II algorithm

T. Vo-Duy[1,2], D. Duong-Gia[1,2], V. Ho-Huu[3], H.C. Vu-Do[1,2], T. Nguyen-Thoi[1,2,*]

[1]*Division of Computational Mathematics and Engineering, Institute for Computational Science, Ton Duc Thang University, Ho Chi Minh City, Vietnam*
[2]*Faculty of Civil Engineering, Ton Duc Thang University, Ho Chi Minh City, Vietnam*
[3]*Faculty of Aerospace Engineering, Delft University of Technology, Delft, The Netherlands*

E-mail addresses: voduytrung@tdt.edu.vn (T. Vo-Duy); duongdungue@gmail.com (D. Duong-Gia); V.HoHuu@tudelft.nl (V. Ho-Huu); vdhuycuong@gmail.com (H.C. Vu-Do); nguyenthoitrung@tdt.edu.vn (T. Nguyen-Thoi)

Abstract

The paper deals with the multi-objective optimization problem of laminated composite beam structures. The objective function is to minimize the weight of the whole laminated composite beam and maximize the natural frequency. The design variables include fiber volume fractions, thickness and fiber orientation angles of layers, in which the fiber volume fractions are taken as continuous design variables with the constraint on manufacturing process while the thickness and fiber orientation angles are considered as discrete variables. The beam structure is subject to the constraint in the natural frequency which must be greater than or equal to a predetermined frequency. For free vibration analysis of the structure, the finite element method is used with the two-node Bernoulli-Euler beam element. For solving the multi-objective optimization problem, the nondominated sorting genetic algorithm II (NSGA-II) is employed. The reliability and effectiveness of the proposed approach are demonstrated through three numerical examples by comparing the current results with those of previous studies in the literature.

Keywords: *Multi-objective optimization, laminated composite beam, nondominated sorting genetic algorithm II (NSGA-II), fiber volume fraction, frequency constraint.*

[*] Corresponding author. Tel.: +84 933 666 226
E-mail addresses: nguyenthoitrung@tdt.edu.vn (Trung Nguyen-Thoi)

1. **Introduction**

Due to various exceptional advantages, composite structures have been widely used in automotive industries, civil infrastructures, and aerospace structures, especially in aircraft and a lot of other engineering applications. One of the primary advantages of composite structures is smaller weight density in comparison with metallic structures. In addition, some composite structures also provide better stiffness compared to metallic structures. Beyond such the advantages, the effective use of composite structures also depends significantly on an optimal design which is the result of solving the single-objective or multi-objective optimization problems with either the lowest weight or the maximum stiffness (for the single-objective cases), or both of them (for the multi-objective cases). However, for the case of laminated composite structures, the optimization design procedure is usually more complex than those associated with isotropic material structures. This is because there is a large number of involved variables and the intrinsic anisotropy behavior of the individual layers in the laminated composite structures [1]. As a result, although there have been a lot of related studies published in the literature, design optimization for laminated composite structures has been still a matter of current research.

Over several decades, the study on design optimization for laminated composite structures like beams and plates is preferred and has attracted a certain attention from many researchers around the world. A lot of these previous studies focused on single-objective optimization in which the fitness functions are usually maximizing fundamental frequency [2–7], or maximizing buckling load [8–13], or maximizing strain energy/stress [14–17], or minimizing weight [18–20], or topology optimization [21,22] while design variables are frequently fiber orientation angles, fiber distribution and thickness of layers.

Recently, Liu [23,24] and Vo-Duy et al. [25] presented a new approach for the lightweight design optimization of laminated composite beams and plates. In this approach, the fiber volume fractions of the layers are considered as design variables. Also, the frequency constraint is taken into account. According to the numerical results in these studies, the fiber volume factions of the layers shown their significant influence on the weight of the laminated composite structures. However, their studies were limited to a single objective, the weight of the laminated structures. Moreover, the design variables in these studies were just focused on either the fiber volume fractions of the layers in Refs. [23,24] or both fiber volume fractions of the layers and the thickness of the layers in Ref. [25].

On the other hand, there have also been some papers conducted for multi-objective optimization of laminated composite structures. For example, Pelletier and Vel [26] studied the multi-objective optimization of fiber reinforced composite materials. Two models with conflicting objectives were carried out in this study. In the first model problem, the objective functions were to maximize the failure load and minimize the mass of a graphite/epoxy laminate subjected to the constraint of biaxial moments. In the second model problem, objective functions were to maximize the hoop rigidity and axial rigidity and minimize the mass of a graphite/epoxy cylindrical pressure vessel subjected to the constraint of the failure pressure which must be greater than a prescribed value. For both models, fiber orientation angles and fiber volume fractions were taken as design variables. In another study, Lee et al. [27] presented a work which aimed to minimize the weight of multilayered composite plates and minimize their maximum displacement. The design variables include the type of fiber, thickness and the fiber orientations of each layer. Vosoughi and Nikoo [28] developed a hybrid method for the maximizing fundamental natural frequency and thermal buckling temperature of laminated composite plates. Only fiber orientation angles are treated as design variables in this study. Recently, Honda et al. [29] examined the trade-off solutions between the mechanical performance and curvatures of reinforcing fibers of laminated composite plates via two conflicting objectives. One is to maximize the fundamental frequency or Tsai-Wu failure criteria and the other is to minimize the curvature of the curvilinear fibers. In this work, the design variables are the coefficients of the shape of the curvilinear fibers.

So far in a general view, it can be seen from the literature that most of the studies related to multi-objective optimization of laminated composite structures focused on considering the optimal solutions related to minimal weight and static characteristic of the structures, and the design variables are either the thickness or fiber volume fraction that are integrated with the fiber orientation angles. There are a few papers, where the trade-off relationship between the weight and the frequency of the laminated composite beams are studied. Moreover, the simultaneous use of all the fiber volume fractions, thickness and fiber orientation angles of layers for multi-objective optimization of laminated composite structures is somewhat still limited.

Under such mentioned research gaps for the multi-objective optimization of laminated composite beam structures and motivated by the studies of Liu [23,24] and our previous work [25] on lightweight design of laminated composite beams and plates under frequency constraint, the present paper hence deals with the multi-objective optimization of laminated composite beams for minimizing the weight of the whole laminated composite beam and maximizing its natural frequency. The design variables are fiber volume fractions, thickness and fiber orientation angles of layers in which the fiber volume fractions are taken as continuous design variables with the constraint on manufacturing process while the thickness and fiber orientation angles are considered as discrete variables. The beam structure is subject to the constraint in the natural frequency which must be greater than or equal to a predetermined frequency. For free vibration analysis of the structure, the finite element method is used with the two-node Bernoulli-Euler beam element. For solving the multi-objective optimization problem, the nondominated sorting genetic algorithm II (NSGA-II) [30] is employed. Three numerical examples are implemented with the presence of Pareto optimal solution set. In addition, the present results are also compared with those of previous study in the literature to demonstrate the reliability and effectiveness of the proposed approach.

The remainder of the paper is organized as follows. Section 2 summarizes the governing equations related to free vibration analysis of the laminated composite beam. Section 3 formulates the multi-objective optimization problem for laminated composite beams. Section 4 briefly presents the NSGA-II algorithm. Section 5 examines some numerical examples, and Section 6 draws some conclusions.

2. Free vibration of laminated composite beams

Consider a laminated composite beam consisting of N layers. The size of the beam is characterized by the length L, the width b and the thickness h. A global coordinate system $Oxyz$ is attached at the center of the beam such that the x-axis is in the longitudinal direction, as shown in Figure 1. Here the bending of the beam on the yz-plane is not considered. In each layer, we denote the fiber orientation angles by $\theta^{(1)}$, $\theta^{(2)}$, $\theta^{(3)}$,...., $\theta^{(N)}$, the fiber volume fractions by r_f^1, r_f^2,..., r_f^N and vertical coordinates of layers by z_0, z_1,..., z_{N-1}, z_N.

Based on a classical beam theory (CBT) or Euler Bernoulli (EB) beam theory where the influence of shear deformation and rotary inertia can be ignored, the displacement field of the laminated composite beam is given by

$$\begin{aligned} u(x,z) &= z\beta_x(x) \\ w(x,z) &= w_0(x) \end{aligned} \quad (1)$$

where u and w are x-direction and z-direction displacements of the beam respectively; β_x is the rotation of the cross section and determined by $\beta_x = \frac{\partial w}{\partial x}$; and w_0 is the z-direction displacement of the beam neutral axis.

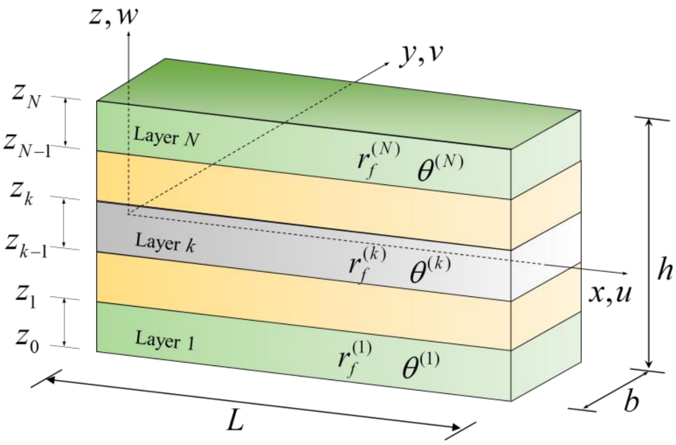

Figure 1. A laminated composite beam.

The relationship between the displacement and strain is expressed by $\varepsilon_x = \frac{\partial u}{\partial x} = z\frac{\partial^2 w}{\partial x^2}$.

Then the stress-strain equations for an element of material in the kth lamina may be written as

$$\sigma_x^{(k)} = \bar{Q}_{11}^{(k)} \varepsilon_x \tag{2}$$

where

$$\bar{Q}_{11}^{(k)} = Q_{11}^{(k)} \cos^4 \theta^{(k)} + 2\left(Q_{12}^{(k)} + 2Q_{66}^{(k)}\right) \sin^2 \theta^{(k)} \cos^2 \theta^{(k)} + Q_{22}^{(k)} \sin^4 \theta^{(k)} \tag{3}$$

with

$$Q_{11}^{(k)} = \frac{E_1^{(k)}}{1 - \nu_{12}^{(k)} \nu_{21}^{(k)}},\ Q_{12}^{(k)} = \frac{\nu_{12} E_2^{(k)}}{1 - \nu_{12}^{(k)} \nu_{21}^{(k)}},\ Q_{66}^{(k)} = G_{12}^{(k)},\ Q_{22}^{(k)} = \frac{E_2^{(k)}}{1 - \nu_{12}^{(k)} \nu_{21}^{(k)}} \tag{4}$$

where $E_1^{(k)}$ and $E_2^{(k)}$ are longitudinal and transverse elastic moduli, respectively; $\nu_{12}^{(k)}$ and $\nu_{21}^{(k)}$ are Poisson constants; $G_{12}^{(k)}$ is strain modulus. These parameters are calculated as [23,31]

$$\begin{aligned}
E_1^{(k)} &= E_f r_f^{(k)} + E_m r_m^{(k)} = E_f r_f^{(k)} + E_m \left(1 - r_f^{(k)}\right) \\
E_2^{(k)} &= \frac{E_f E_m}{E_f r_m^{(k)} + E_m r_f^{(k)}} = \frac{E_f E_m}{E_f \left(1 - r_f^{(k)}\right) + E_m r_f^{(k)}} \\
\nu_{12}^{(k)} &= \nu_{21}^{(k)} = \nu_f r_f^{(k)} + \nu_m r_m^{(k)} = \nu_f r_f^{(k)} + \nu_m \left(1 - r_f^{(k)}\right) \\
G_{12} &= \frac{G_f G_m}{G_f r_m^{(k)} + G_m r_f^{(k)}} = \frac{G_f G_m}{G_f \left(1 - r_f^{(k)}\right) + G_m r_f^{(k)}} \\
G_f &= \frac{E_f}{2\left(1 + \nu_f\right)}, G_m = \frac{E_m}{2\left(1 + \nu_m\right)}
\end{aligned} \tag{5}$$

where E_f is the elastic modulus of fiber; E_m is modulus of matrix; ν_f is Poisson constant of fiber and ν_m is Poisson constant of matrix.

The governing equation for free vibration of the laminated composite beam can be obtained by using the Hamilton's principle

$$\delta\int_{t_0}^{t_1}\left[\frac{1}{2}\int_V \sigma_x^{(k)}\varepsilon_x \,\mathrm{d}V - \frac{1}{2}\int_V \rho^{(k)}\left(\dot{u}^2+\dot{w}^2\right)\mathrm{d}V\right]\mathrm{d}t = 0 \tag{6}$$

where $\rho^{(k)}$ is the mass density of the kth layer and expressed as follows

$$\rho^{(k)} = r_f^{(k)}\rho_f + \left(1-r_f^{(k)}\right)\rho_m \tag{7}$$

where ρ_f and ρ_m are the density of fiber and matrix, respectively.

Using the finite element method, the overall system equations of motion can be expressed as

$$\mathbf{M}\ddot{\mathbf{d}} + \mathbf{K}\mathbf{d} = 0 \tag{8}$$

where $\mathbf{d}$ is the nodal displacement vector; $\ddot{\mathbf{d}}$ is the second-order derivative with respect to time of $\mathbf{d}$; $\mathbf{M}$ and $\mathbf{K}$ are the global mass and stiffness matrices which are assembled, respectively, from elemental stiffness matrix ($\mathbf{K}^e$) and elemental mass matrix ($\mathbf{M}^e$), given by

$$\mathbf{K}^e = \frac{D_{11}}{l_e^3}\begin{bmatrix} 12 & 6l_e & -12 & 6l_e \\ & 4l_e^2 & -6l_e & 2l_e^2 \\ & & 12 & -6l_e \\ \text{sym.} & & & 4l_e^2 \end{bmatrix};\ \mathbf{M}^e = \frac{I_1 l_e}{420}\begin{bmatrix} 156 & 22l_e & 54 & -13l_e \\ & 4l_e^2 & 13l_e & -3l_e^2 \\ & & 156 & -22l_e \\ \text{sym.} & & & 4l_e^2 \end{bmatrix} \tag{9}$$

where l_e is the length of the eth element and D_{11} and I_1 are defined by

$$D_{11} = \frac{1}{3}\sum_{k=0}^{N} b\overline{Q}_{11}^{(k)}\left(z_k^3 - z_{k-1}^3\right);\ I_1 = \sum_{k=0}^{N} b\rho^{(k)}\left(z_k - z_{k-1}\right) \tag{10}$$

The natural frequency ω and mode shape f of the beam are obtained by solving the eigenvalue problem which is derived from Equation (8) as follows

$$(\mathbf{K} - w^2\mathbf{M})f = 0 \tag{11}$$

3. Formulation of the multi-objective optimization problem

In this study, the objective functions of multi-objective optimization problem are to minimize the weight and maximize the first natural frequency of a laminated composite beam. The optimization problem has a constraint on the first frequency that must be larger than a predefined value by designer. The mass of the laminated composite beam is strongly influenced by thickness and fiber volume fractions of layers while the first frequency of the laminated composite beam is significantly influenced not only by thickness and fiber volume fractions, but also by fiber orientation angles of layers. This paper hence considers all variables including thickness, fiber volume fractions and fiber orientation angles of layers as design variables. In addition, to investigate in detail, the effect of these variables on the Pareto-optimal solution, three models with various design variables are suggested for the multi-objective optimization problem as follows.

+ Model 1: only fiber volume fractions of layers are the design variables:

$$\begin{aligned}
&\text{Minimum} && mass\left(\mathbf{r}_f\right) = \sum_{k=1}^{N} \rho^{(k)}\left(r_f^{(k)}\right) \times A_k \times t^{(k)} \\
&\text{Maximum} && freq\left(\mathbf{r}_f\right) \\
&\text{subject to} && freq\left(\mathbf{r}_f\right) \geq \underline{f}_1 \\
& && 0 \leq r_f^{(k)} \leq r_f^{\max}, \quad k = 1,...,N
\end{aligned} \tag{12}$$

+ Model 2: fiber volume fractions and thickness of layers are the design variables:

$$\begin{aligned}
&\text{Minimum} && mass\left(\mathbf{r}_f, \mathbf{t}\right) = \sum_{k=1}^{N} \rho^{(k)}\left(r_f^{(k)}\right) \times A_k \times t^{(k)} \\
&\text{Maximum} && freq\left(\mathbf{r}_f, \mathbf{t}\right) \\
&\text{subject to} && freq\left(\mathbf{r}_f, \mathbf{t}\right) \geq \underline{f}_1 \\
& && 0 \leq r_f^{(k)} \leq r_f^{\max} \\
& && t_{\text{low}} \leq t^{(k)} \leq t_{\text{up}}, \quad k = 1,...,N
\end{aligned} \tag{13}$$

+ Model 3: fiber volume fractions, thickness and fiber orientation angles of layers are the design variables:

$$\begin{aligned}
&\text{Minimum} && mass\left(\mathbf{r}_f, \mathbf{t}\right) = \sum_{k=1}^{N} \rho^{(k)}\left(r_f^{(k)}\right) \times A_k \times t^{(k)} \\
&\text{Maximum} && freq\left(\mathbf{r}_f, \mathbf{t}, \boldsymbol{\theta}\right) \\
&\text{subject to} && freq\left(\mathbf{r}_f, \mathbf{t}, \boldsymbol{\theta}\right) \geq \underline{f}_1 \\
& && 0 \leq r_f^{(k)} \leq r_f^{\max} \\
& && t_{\text{low}} \leq t^{(k)} \leq t_{\text{up}}, \qquad k = 1,\ldots,N \\
& && -90^0 \leq \theta^{(k)} \leq 90^0
\end{aligned} \tag{14}$$

where $mass\left(\mathbf{r}_f, \mathbf{t}\right)$ and $freq\left(\mathbf{r}_f, \mathbf{t}\right)$ are the mass and first frequency of the beam, respectively; $\mathbf{r}_f$, $\mathbf{t}$, $\boldsymbol{\theta}$ are the design variable vectors of fiber volume fractions $r_f^{(k)}$, thickness $t^{(k)}$ and fiber orientation angle $\theta^{(k)}$ of layers, respectively; $\rho^{(k)}\left(r_f^{(k)}\right)$ and A_k are the mass density and the area of the kth layer, respectively; $\underline{f_1}$ is the lower bound of the first frequency; t_{low} and t_{up} are respectively the lower and upper bounds of $t^{(k)}$; N is the total number of layers; and $r_f^{\max}$ is the maximum of r_f in a lamina. In manufacturing, it should be noted that the maximum value of r_f depends on the arrangement of fiber in the matrix. As mentioned in references [31,32], the value of $r_f^{\max}$ can be either 0.7854 if the fiber arrangement is a square array as described in Figure 2a or 0.9069 if the fiber arrangement is a hexagonal array as shown in Figure 2b.

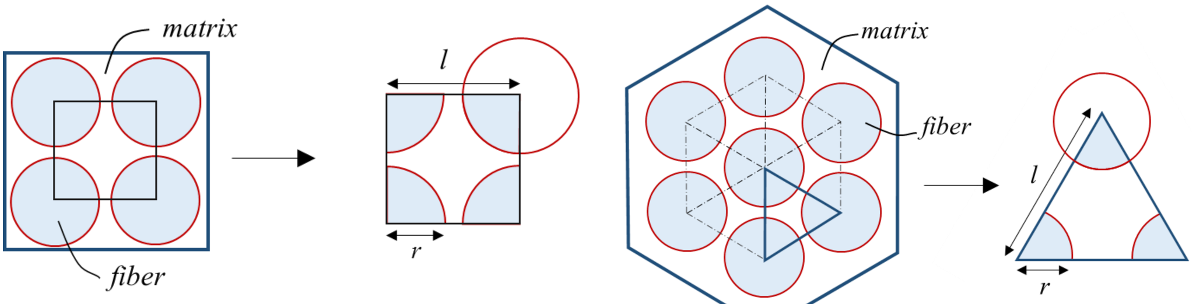

$$r_f = \frac{\text{Area of fiber}}{\text{Area of matrix}} = \frac{4\dfrac{\pi r^2}{4}}{l^2} = \frac{\pi r^2}{l^2},$$

$$r_f^{\max} = \frac{\pi r^2}{(2r)^2} = \frac{\pi}{4} = 0.7854$$

(a)

$$r_f = \frac{\text{Area of fiber}}{\text{Area of matrix}} = \frac{3\dfrac{\pi r^2}{6}}{\dfrac{1}{2} l.l \sin\left(\dfrac{\pi}{3}\right)} = \frac{2\pi r^2}{\sqrt{3} l^2},$$

$$r_f^{\max} = \frac{2\pi r^2}{\sqrt{3} l^2} = \frac{2\pi r^2}{\sqrt{3}.(2r)^2} = \frac{\pi}{2\sqrt{3}} = 0.9069$$

(b)

Figure 2. Fiber arrangements. (a) Square array; (b) Hexagonal array.

4. NSGA-II algorithm

Unlike the single-objective optimization problem which provides only a single optimal solution, the multi-objective optimization problem will provide a set of points known as Pareto optimal set which represents the trade-off solutions between conflicting objectives. To obtain the Pareto-optimal solutions, a number of techniques have been proposed in the literature [33] in which the multi-objective evolutionary algorithms (MOEAs) such as NSGA-II [30], SPEA-II [34], and MOEA/D [35] gained much attention from the researchers due to their effectiveness and easy implementation. Among these attended MOEAs, the NSGA-II is considered as one of the most powerful methods. This algorithm is an improved version of NSGA [36] developed from the well-known genetic algorithm ([37–40]) and non-dominated sorting concept by Goldberg [41]. In the past decade, the NSGA-II has been improved and widely applied in design optimization of various problems (see, for example, references [42–45]) and also in design optimization of laminated composite plate structures [26,29]. In this paper, the NSGA-II algorithm is used to solve a the multi-objective optimization problem related to the laminated composite beam presented in section 3. The brief description of the algorithm is presented below.

(1) Generate an initial population P_0 with N solutions is randomly.

(2) Create an offspring population Q_t using binary tournament selection based on crowding-comparison operator, crossover and mutation performed on the parent population (P_t), where subscript "t" denotes the number of generations. The offspring population and its parent population are then combined to produce the entire population R_t.

(3) Perform a fast nondominated sorting approach on the entire population R_t to identify different nondominated fronts of objective functions F_1, F_2, etc.

(4) Create a new parent population (P_{t+1}) of size N from the obtained fronts (F_i).

(5) Repeat the process until the maximum number of iterations is reached.

For more details of the above procedure, the readers are encouraged to refer to the original paper [30].

5. Numerical examples

In this section, numerical results of optimal design for a symmetric laminated composite beam structure are presented. The beam was previously studied by Liu [23] for single-objective optimization. The geometric parameters of the laminated composite beam are given by: length L = 14.4 m, width b = 0.3 m and height h = 0.48 m. The beam has the same number of layers ($N = 8$) and the same material properties as given by Liu [23], i.e., the fiber material $E_f = 294\,\text{GPa}$, $v_f = 0.2$, $\rho_f = 1.81\,\text{g/cm}^3$ and the matrix material $E_m = 4.2\,\text{GPa}$, $v_m = 0.3$, $\rho_m = 1.24\,\text{g/cm}^3$. The laminated composite beam has two kinds of fiber orientation angles which include $[0^0/90^0/45^0/\text{-}45^0]_S$ and $[45^0/0^0/90^0/\text{-}45^0]_S$.

The optimization problem is investigated with three different models as already mentioned in Section 3. In all models, the fiber volume fractions of layers are treated as the continuous design variables and its upper bound, r_{max}, is set to be 0.9069. In addition, in the first model, the thickness of layers and fiber orientation angles are fixed and same as those in [23], i.e, $t^{(k)}$ = 6 mm (k = 1,...,8) and two kinds of fiber orientation angles including $[0^0/90^0/45^0/\text{-}45^0]_S$ and $[45^0/0^0/90^0/\text{-}45^0]_S$. In the second model, the fiber orientation angles of layers are kept constant similarly as in the first model while thicknesses of layers are treated as the discrete design variables which are integers in the range of [1, 20] (unit: mm). In the third model, both thickness and fiber orientation angles of layers are considered as discrete design variables in which the constraint of thickness the same as considered in the second model and the fiber orientation angles of layers are integers in the range of [-90^0, 90^0].

In each model, the optimization problem is conducted with four different boundary conditions: fixed–fixed, fixed–free, fixed–pinned and pinned–pinned, and the NSGA-II method is applied with the population size of 50 and maximum number of iterations of 100.

5.1 Solution of frequencies of laminated composite beam using finite element method

The frequencies of the laminated composite beam are determined by using two-node Bernoulli-Euler beam element. The accuracy and reliability of the programing by this finite element analysis is demonstrated through the numerical results of the case of [0/90/45/-45]s laminated composite beam whose fibre volume fractions are $r_f^{(k)}$ = 50% (k = 1, 2, ..., 8). The beam structure is divided into 16 beam elements of equal lengths. The first four squares of frequencies (ω^2) of the beam with four different boundary conditions are provided in Table 1 in comparison with the analytical solutions. It can be seen from the table an excellent agreement between results. The results illustrated clearly the high accuracy and reliability of the numerical analysis for determining the frequencies of the laminated composite beam, and hence this numerical analysis can be ready to integrate effectively with the NSGA-II for finding the optimal solutions of the multi-objective optimization problems.

Table 1. The first four frequencies ω^2 (Hz^2) of the laminated composite beam.

Boundary condition	Method	Mode 1	Mode 2	Mode 3	Mode 4
pinned-pinned	Analytical [23]	2862	45,795	231,838	732,722
	Present	2862	45,795	231,840	732,746
fixed-fixed	Analytical [23]	14,708	111,761	429,514	1,173,680
	Present	14,708	111,761	429,522	1,173,740
fixed-free	Analytical [23]	363	14,266	111,848	429,503
	Present	363	14,266	111,849	429,511
fixed-pinned	Analytical [23]	6985	73,355	319,324	933,803
	Present	6985	73,355	319,329	933,841

5.2. Solution of multi-objective optimization problem: Model 1

Figures from Figure 3 to Figure 6 show the Pareto-optimal solutions of the laminated composite beams for different boundary conditions where the horizontal and vertical axes represent the weight and first frequency, respectively. For each beam and each boundary condition, the optimal solution corresponding with the lowest frequency is provided in Table 2, Table 3, Table 4 and Table 5 in comparison with the single-objective optimization solution obtained by Liu [23].

As can be seen from Table 2 to Table 5, the obtained weights by the present approach are the same as those by Liu [23] in almost cases. A little difference is observed only for the case of [$45^0/0^0/90^0/-45^0$] beam with fixed-free boundary condition. This is because the fiber volume fraction varies from 0 to 1 in Liu's study while it varies from 0 to 0.9060 in the present study which is more accurate as shown in geometrical analysis of Figure 2.

As can be observed in Figures from Figure 3 to Figure 6, the Pareto-optimal curves are different for two beams having different fiber orientations. Particularly, for the case of [$0^0/90^0/45^0/-45^0$]s beam, the Pareto-optimal solutions are seen to be nearly linear for all four various boundary conditions. While for the case of [$45^0/0^0/90^0/-45^0$]s beam, these curves are nonlinear for all four various boundary conditions. Also, it can be seen that the best weights corresponding to the lowest frequency of the case of [$45^0/0^0/90^0/-45^0$]s beam are always greater than those of the case of [$0^0/90^0/45^0/-45^0$]s beam.

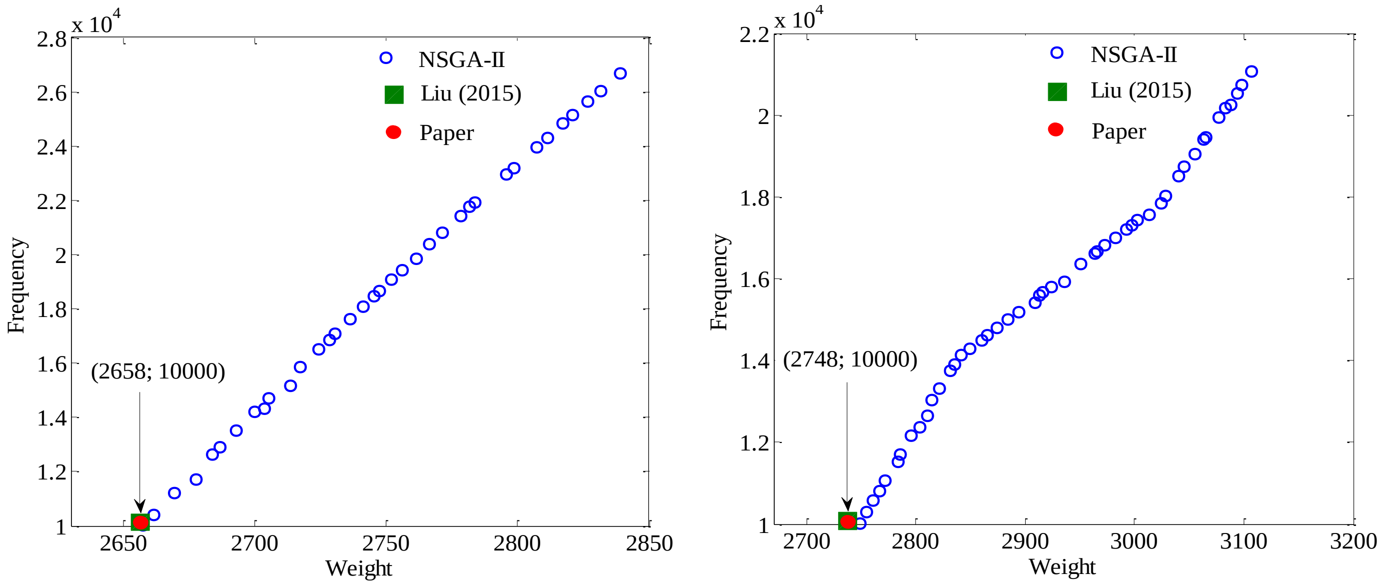

(a) [$0^0/90^0/45^0/-45^0$]s (b) [$45^0/0^0/90^0/-45^0$]s

Figure 3. Pareto-optimal solutions of fixed–fixed beam for model 1.

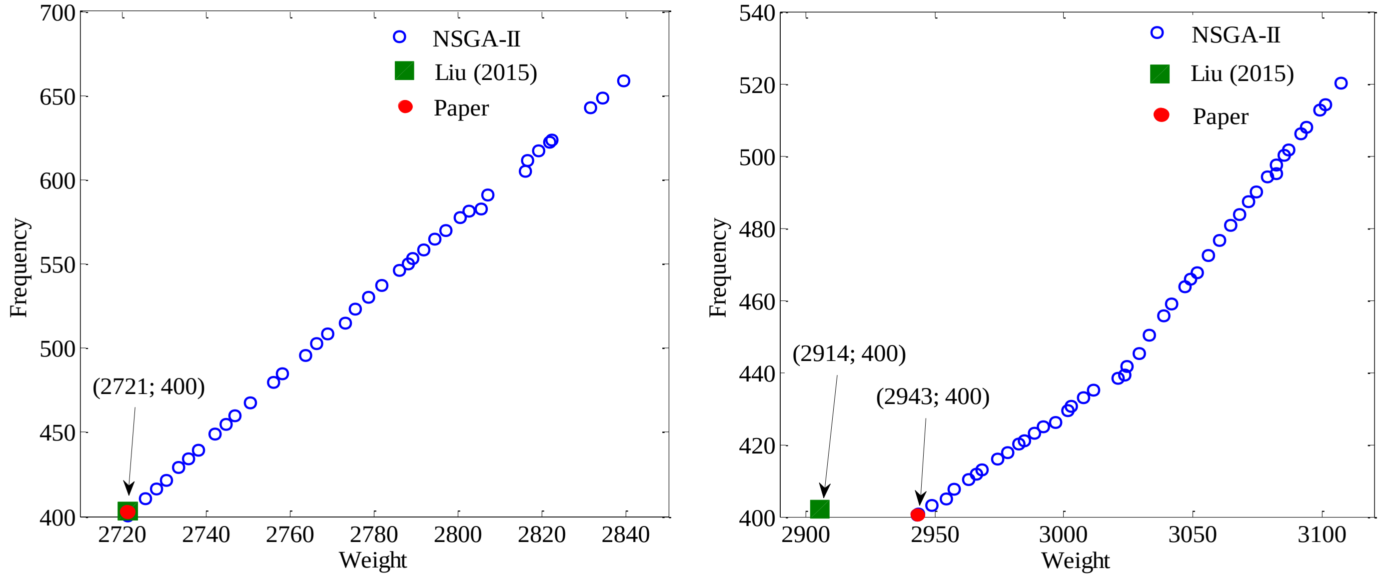

(a) [0⁰/90⁰/45⁰/-45⁰]s (b) [45⁰/0⁰/90⁰/-45⁰]s

Figure 4. Pareto-optimal solutions of fixed–free beam for model 1.

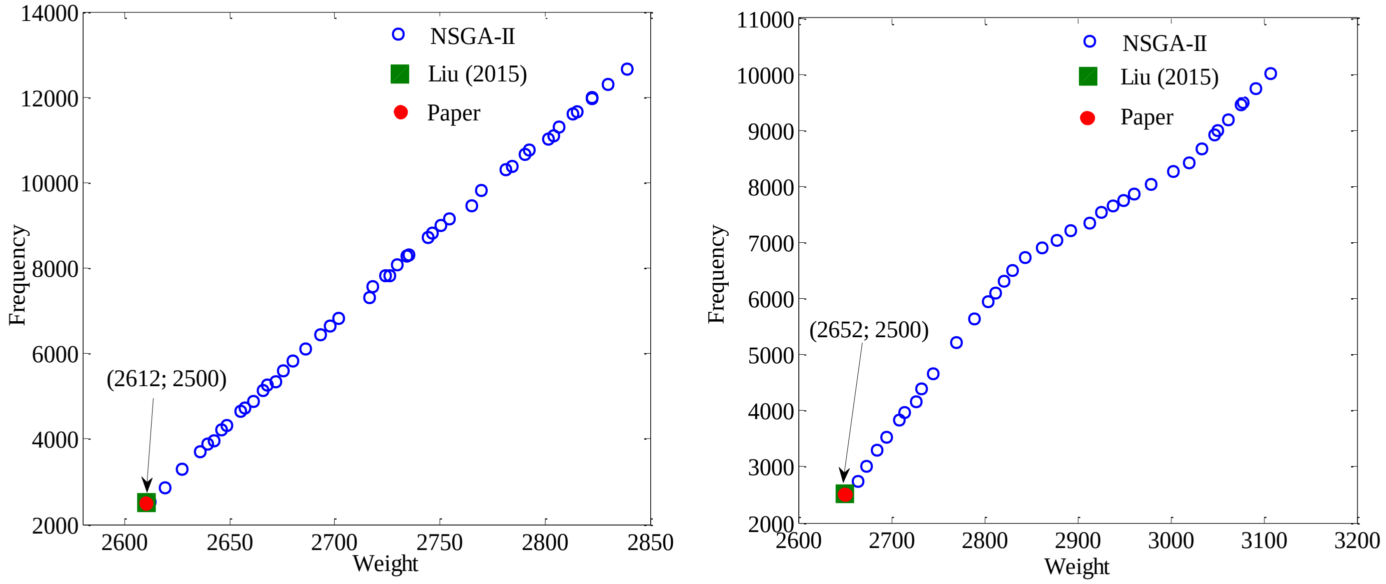

(a) [0⁰/90⁰/45⁰/-45⁰]s (b) [45⁰/0⁰/90⁰/-45⁰]s

Figure 5. Pareto-optimal solutions of fixed–pinned beam for model 1.

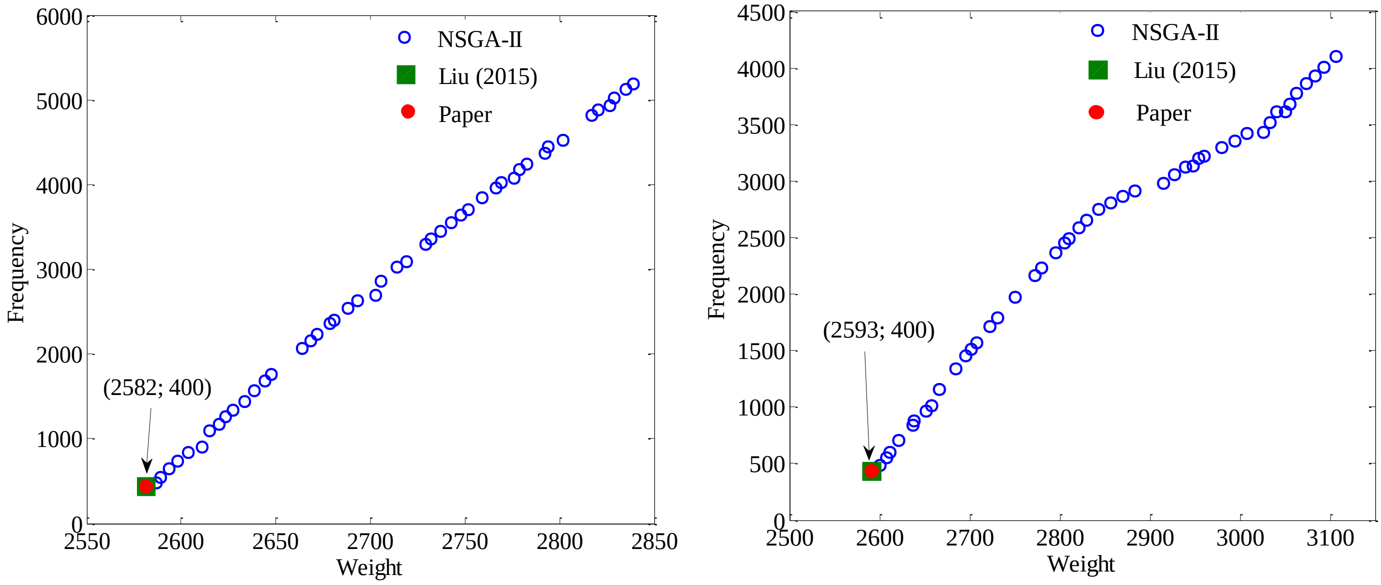

(a) $[0^0/90^0/45^0/-45^0]$s (b) $[45^0/0^0/90^0/-45^0]$s

Figure 6. Pareto-optimal solutions of pinned- pinned beam for model 1.

Table 2. Optimal design results of the fixed-fixed beam for model 1

Fibre orientation	Method	Fiber volume fraction (%)				Weight (kg)	Frequency (Hz^2)
		$r_f^{(1)}$	$r_f^{(2)}$	$r_f^{(3)}$	$r_f^{(4)}$		
$[0^0/90^0/45^0/-45^0]$s	Ref. [23]	29.2	0	0	0	2658	10000
	NSGA-II	29.2	0	0	0	2658	10000
$[45^0/0^0/90^0/-45^0]$s	Ref. [23]	0	59.9	0	0	2748	10000
	NSGA-II	0	60.03	0	0	2748	10000

Table 3. Optimal design results of the fixed–free beam for model 1

Fibre orientation	Method	Fiber volume fraction (%)				Weight (kg)	Frequency (Hz^2)
		$r_f^{(1)}$	$r_f^{(2)}$	$r_f^{(3)}$	$r_f^{(4)}$		
$[0^0/90^0/45^0/-45^0]$s	Ref. [23]	50.7	0	0	0	2721	400
	NSGA-II	50.7	0	0	0	2721	400
$[45^0/0^0/90^0/-45^0]$s	Ref. [23]	16	100	0	0	2914	400
	NSGA-II	34.95	90.69	0	0	2943	400

Table 4. Optimal design results of the fixed–pinned beam for model 1

Fibre orientation	Method	Fiber volume fraction (%)				Weight (kg)	Frequency (Hz^2)
		$r_f^{(1)}$	$r_f^{(2)}$	$r_f^{(3)}$	$r_f^{(4)}$		
$[0^0/90^0/45^0/-45^0]$s	Ref. [23]	13.7	0	0	0	2612	2500
	NSGA-II	13.8	0	0	0	2612	2500

[$45^0/0^0/90^0/-45^0$]s	Ref. [23]	0	27	0	0	2652	2500
	NSGA-II	0	27.6	0	0	2652	2500

Table 5. Optimal design results of the pinned –pinned beam for model 1

Fibre orientation	Method	Fiber volume fraction (%)				Weight (kg)	Frequency (Hz^2)
		$r_f^{(1)}$	$r_f^{(2)}$	$r_f^{(3)}$	$r_f^{(4)}$		
[$0^0/90^0/45^0/-45^0$]s	Ref. [23]	3.7	0	0	0	2582	400
	NSGA-II	4	0	0	0	2582	400
[$45^0/0^0/90^0/-45^0$]s	Ref. [23]	0	7.3	0	0	2593	400
	NSGA-II	0	7.96	0	0	2593	400

5.3. Solution of multi-objective optimization problem: Model 2

The Pareto-optimal solutions of two laminated composite beams for various boundary conditions are shown in Figure 7, Figure 8, Figure 9 and Figure 10. For the purpose of comparison, the corresponding Pareto-optimal solutions in model 1 are also illustrated simultaneously in these figures. It can be observed from these figures that the Pareto-optimal solution line in model 2 locates higher than that in model 1. It means that model 2 yields better results than the model 1. For example, as can be seen in Figure 7a, the weight of optimal structure in model 2 (1645 kg - design point A) is less than that of the model 1 (2658 kg - design point C) while the frequencies are the same (10000 Hz). Also, in the same mass (close to 2658kg), model 2 has frequency 26539 Hz (design point B) greater than that of the model 1 (10000 Hz – design point C). In Figures from Figure 8 to Figure 10, the same results in comparison are shown.

Tables from Table 6 to Table 9 provide the fiber volume fractions and thickness of the layers corresponding with design points A, B, C in Figures from Figure 7 to Figure 10. It can be seen that the total thicknesses in design points A and B are smaller than that in design point C. In contrast, the fiber volume fractions of each layer of design points A and B are much larger than that of the design point C.

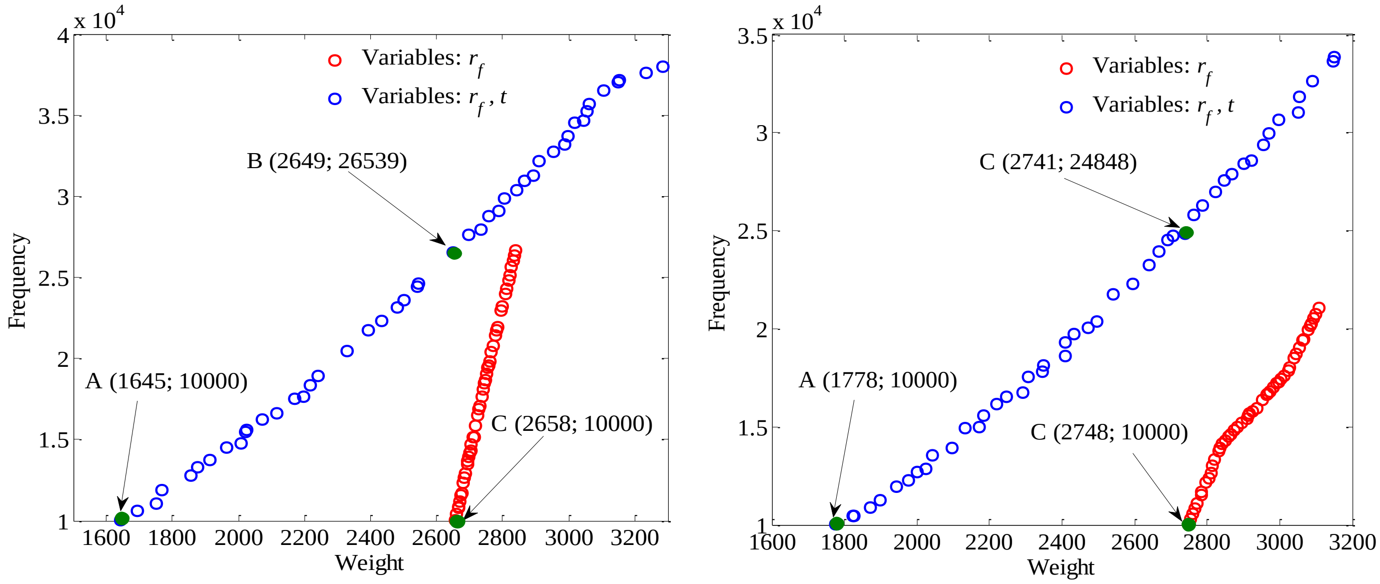

(a) [$0^0/90^0/45^0/-45^0$]s (b) [$45^0/0^0/90^0/-45^0$]s

Figure 7. Pareto-optimal solutions of fixed–fixed beam for model 2 and model 1

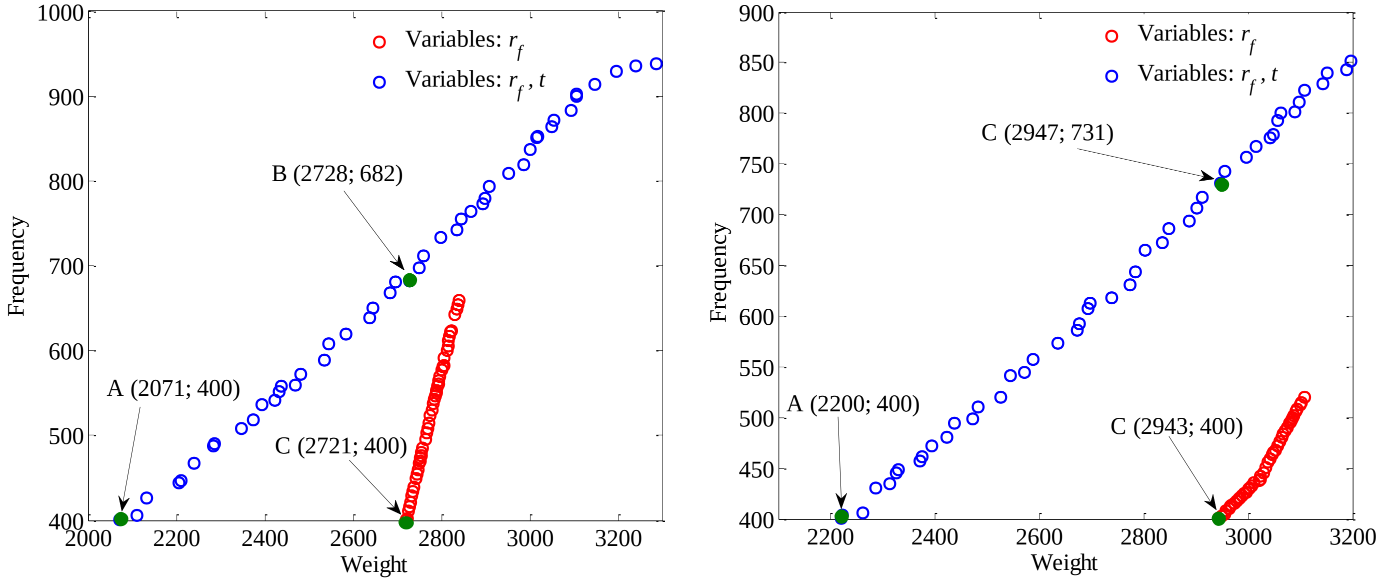

(a) [$0^0/90^0/45^0/-45^0$]s (b) [$45^0/0^0/90^0/-45^0$]s

Figure 8. Pareto-optimal solutions of fixed–free beam for model 2 and model 1.

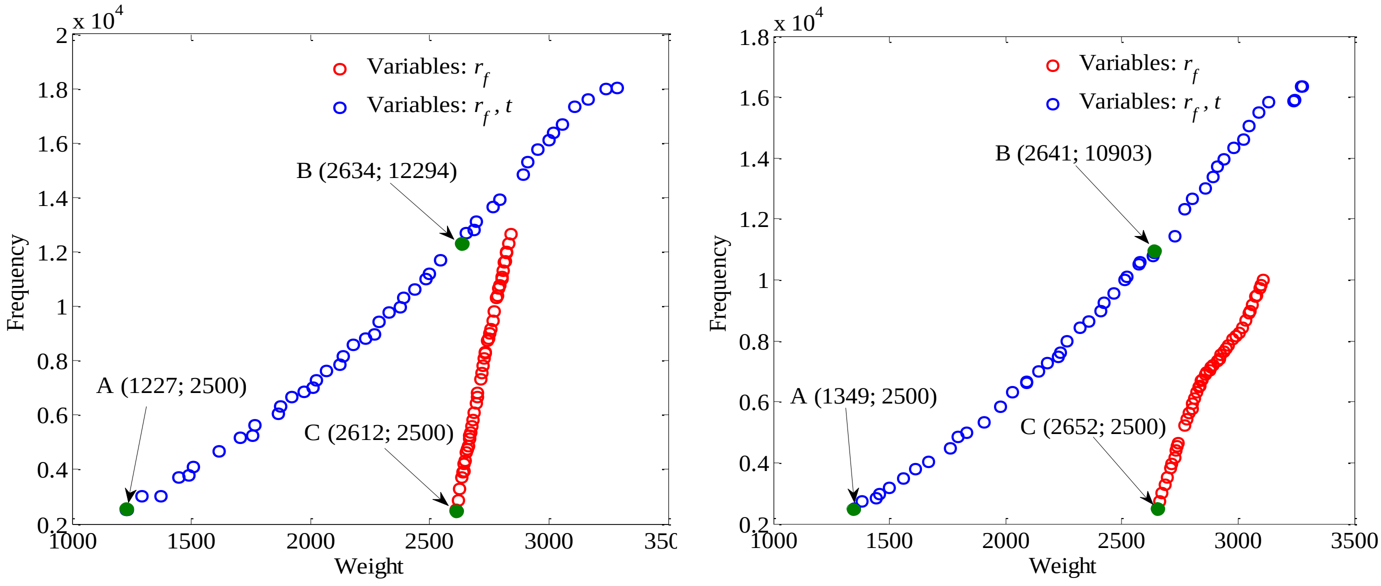

(a) $[0^0/90^0/45^0/-45^0]$s (b) $[45^0/0^0/90^0/-45^0]$s

Figure 9. Pareto-optimal solutions of fixed–pinned beam for model 2 and model 1.

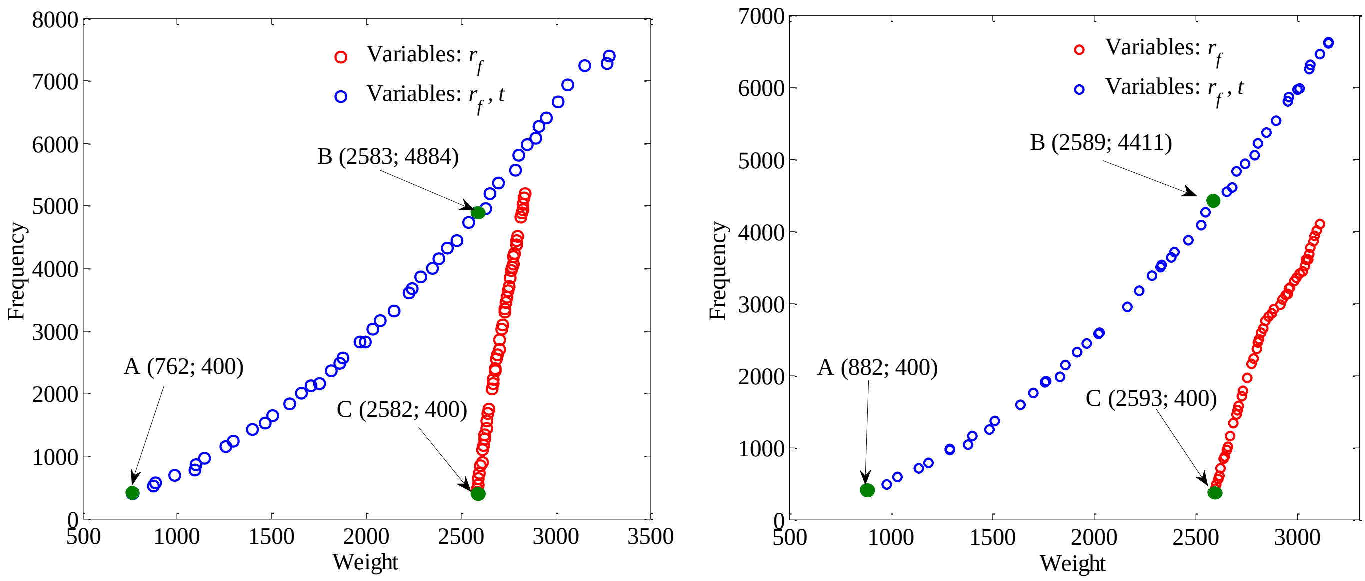

(a) $[0^0/90^0/45^0/-45^0]$s (b) $[45^0/0^0/90^0/-45^0]$s

Figure 10. Pareto-optimal solutions of pinned- pinned beam for model 2 and model 1.

Table 6. Optimal design results of the laminated composite beams (fixed–fixed) for model 2

Fibre orientation	Design variable	Thickness (mm)				Fiber volume fraction (%)				Weight (kg)	Frequency (Hz^2)
		t_1	t_2	t_3	t_4	$r_f^{(1)}$	$r_f^{(2)}$	$r_f^{(3)}$	$r_f^{(4)}$		
$[0^0/90^0/45^0/-45^0]$s	r_f (C)	6	6	6	6	29.2	0	0	0	2658	10000
	t, r_f (A)	6	5	1	1	85.39	0	0	0	1645	10000
	t, r_f (B)	9	6	4	2	90	0	0	0	2649	26539

Fibre orientations	Design variable	t_1	t_2	t_3	t_4	$r_f^{(1)}$	$r_f^{(2)}$	$r_f^{(3)}$	$r_f^{(4)}$	Weight (kg)	Frequency (Hz^2)
$[45^0/0^0/90^0/-45^0]$s	r_f (C)	6	6	6	6	0	60.03	0	0	2748	10000
	t, r_f(A)	1	6	3	4	18.65	90.69	0	0	1778	10000
	t, r_f(B)	1	8	5	8	35.86	90.69	0	2.22	2741	28484

Table 7. Optimal design results of the laminated composite beams (fixed–free) for model 2

Fibre orientations	Design variable	Thickness (mm)				Fiber volume fraction (%)				Weight (kg)	Frequency (Hz^2)
		t_1	t_2	t_3	t_4	$r_f^{(1)}$	$r_f^{(2)}$	$r_f^{(3)}$	$r_f^{(4)}$		
$[0^0/90^0/45^0/-45^0]$s	r_f (C)	6	6	6	6	50.7	0	0	0	2721	400
	t, r_f(A)	8	1	6	1	90.69	0	0	0	2071	400
	t, r_f(B)	11	2	6	2	87.96	1.32	0	0	2728	682
$[45^0/0^0/90^0/-45^0]$s	r_f (C)	6	6	6	6	34.95	90.69	0	0	2943	400
	t, r_f(A)	1	8	7	1	84.85	90.69	0	0	2220	400
	t, r_f(B)	1	10	9	3	73.09	90.69	0	0	2947	731

Table 8. Optimal design results of the laminated composite beams (fixed–pinned) for model 2

Fibre orientation	Design variable	Thickness (mm)				Fiber volume fraction (%)				Weight (kg)	Frequency (Hz^2)
		t_1	t_2	t_3	t_4	$r_f^{(1)}$	$r_f^{(2)}$	$r_f^{(3)}$	$r_f^{(4)}$		
$[0^0/90^0/45^0/-45^0]$s	r_f (C)	6	6	6	6	13.7	0	0	0	2612	2500
	t, r_f(A)	6	1	1	1	89.02	0	0	0	1227	2500
	t, r_f(B)	11	1	4	4	90.69	0	0	0	2634	12294
$[45^0/0^0/90^0/-45^0]$s	r_f (C)	6	6	6	6	0	27	0	0	2652	2500
	t, r_f(A)	1	4	1	5	1.3	86.45	0	0	1349	2500
	t, r_f(B)	1	8	2	10	39.97	90.64	0	2.88	2641	10930

Table 9. Optimal design results of the laminated composite beams (pinned- pinned) for model 2

Fibre orientation	Design variable	Thickness (mm)				Fiber volume fraction (%)				Weight (kg)	Frequency (Hz^2)
		t_1	t_2	t_3	t_4	$r_f^{(1)}$	$r_f^{(2)}$	$r_f^{(3)}$	$r_f^{(4)}$		
$[0^0/90^0/45^0/-45^0]$s	r_f (C)	6	6	6	6	3.7	0	0	0	2582	400
	t, r_f(A)	3	1	1	1	80.86	0	0	0	762	400
	t, r_f(B)	10	6	2	2	89.42	0	0	0	2583	4884
$[45^0/0^0/90^0/-45^0]$s	r_f (C)	6	6	6	6	0	7.3	0	0	2593	400
	t, r_f(A)	1	2	3	1	87.89	90.35	0	0	882	400
	t, r_f(B)	1	9	2	8	89.50	90.69	0	0	2589	4411

5.4. Solution of multi-objective optimization problem: Model 3

The obtained Pareto-optimal solutions of beams for various boundary conditions are shown in Figure 11, Figure 12, Figure 13 and Figure 14. Similarly, for the purpose of comparison, the corresponding Pareto-optimal solutions in model 2 are also shown in these figures. It can be seen that the fiber orientation also affects the optimal design results. In all cases of boundary conditions, the results of model 3 corresponding three design variables are better than the solutions of model 2 with fixed fiber orientations.

Tables from Table 10 to Table 13 list the values of specific design points which have the smallest frequency on Pareto-optimal solutions of Figures from Figure 11 to Figure 14. As can be seen from these tables that model 3 yields different optimal solutions with those of model 2 and it always gives the smallest weight corresponding with the same frequency (1000 Hz). This reveals that fiber orientations angles have a useful effect on the Pareto-optimal solutions.

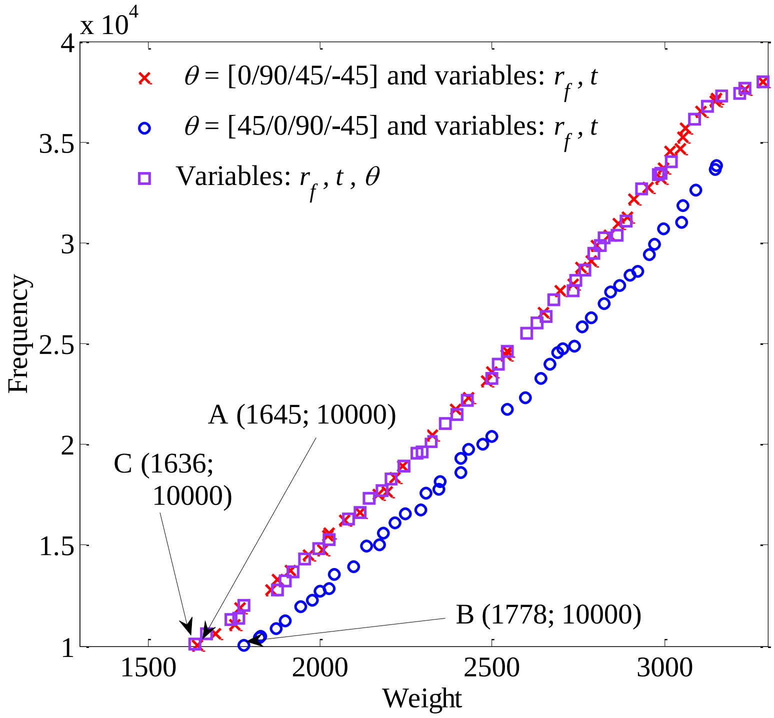

Figure 11. Pareto-optimal solutions of fixed–fixed beam for model 3 and model 2.

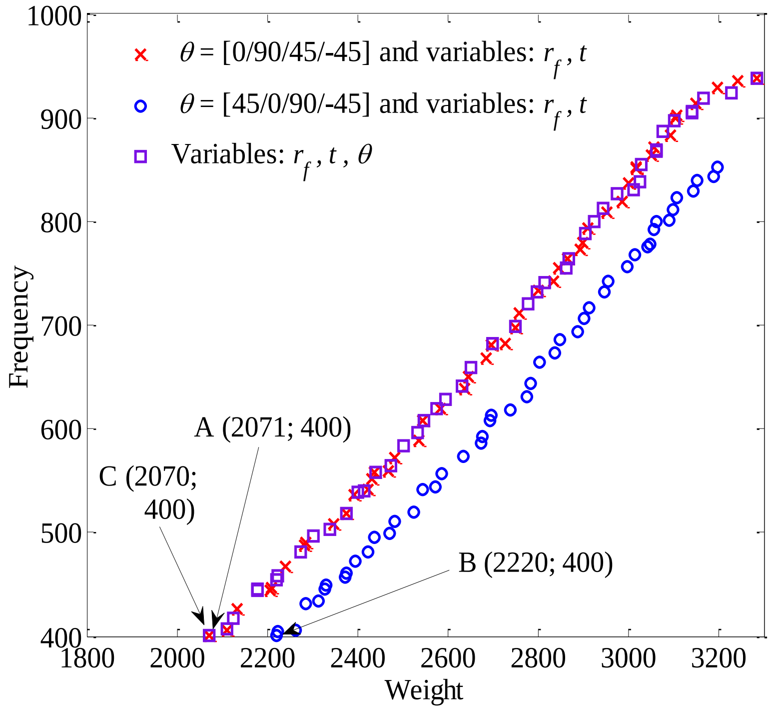

Figure 12. Pareto-optimal solutions of fixed–free beam for model 3 and model 2.

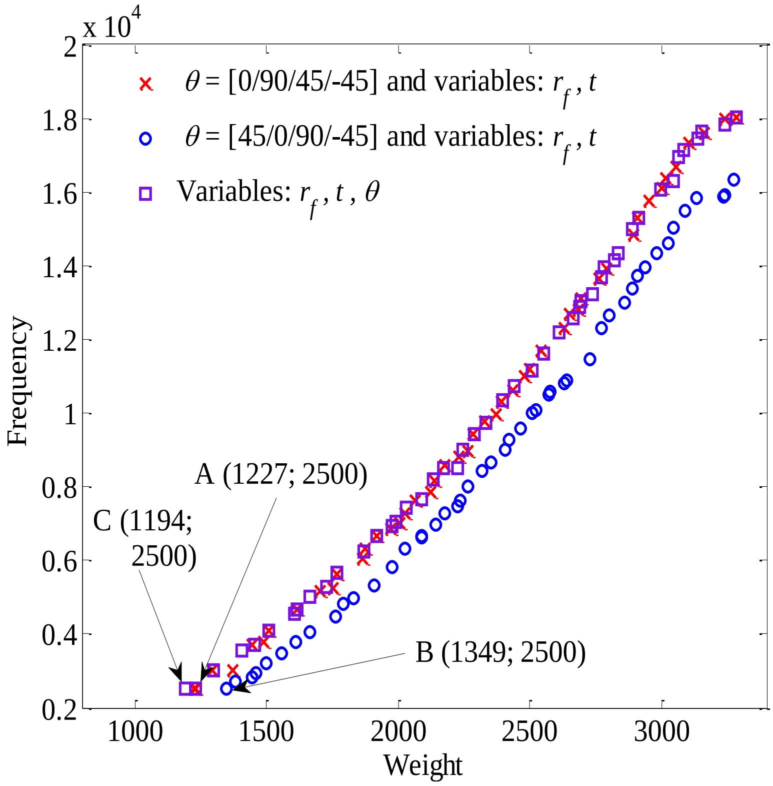

Figure 13. Pareto-optimal solutions of fixed–pinned beam for model 3 and model 2.

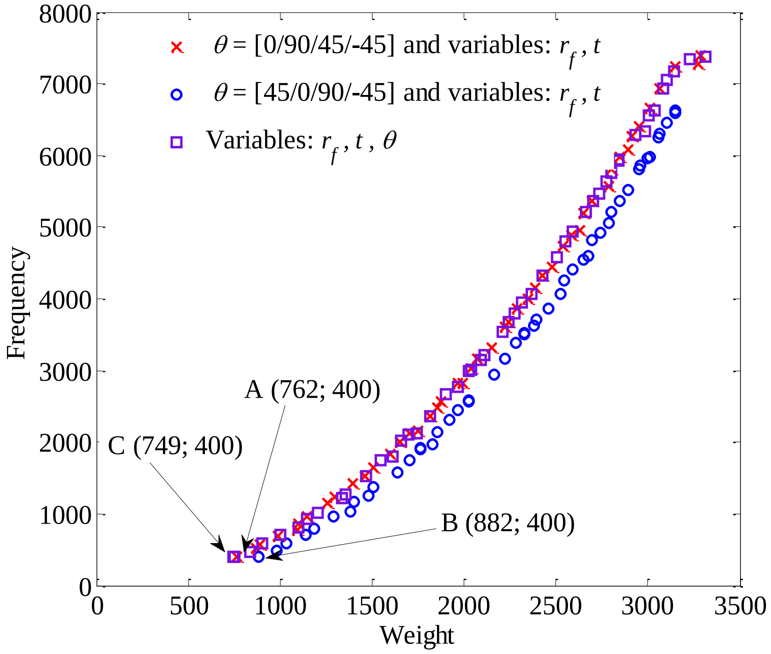

Figure 14. Pareto-optimal solutions of pinned- pinned beam for model 3 and model 2.

Table 10. Optimal design results of the laminated composite beams (fixed–fixed) for model 3

Design variable	Thickness (mm)				Fibre orientation (^{0})				Fiber volume fraction (%)				Weight (kg)	Frequency (Hz^2)
	t_1	t_2	t_3	t_4	θ_1	θ_2	θ_3	θ_4	$r_f^{(1)}$	$r_f^{(2)}$	$r_f^{(3)}$	$r_f^{(4)}$		
t, r_f [$0^0/90^0/45^0/-45^0$]s (A)	6	5	1	1	0	90	45	-45	85.39	0	0	0	1645	10000
t, r_f [$45^0/0^0/90^0/-45^0$]s (B)	1	6	3	4	45	0	90	-45	18.65	90.69	0	0	1778	10000
t, r_f and θ (C)	5	2	2	4	0	-2	-60	-44	90.69	19.75	0	0	1636	10000

Table 11. Optimal design results of the laminated composite beams (fixed–free) for model 3

Design variable	Thickness (mm)				Fibre orientation (^{0})				Fiber volume fraction (%)				Weight (kg)	Frequency (Hz^2)
	t_1	t_2	t_3	t_4	θ_1	θ_2	θ_3	θ_4	$r_f^{(1)}$	$r_f^{(2)}$	$r_f^{(3)}$	$r_f^{(4)}$		
t, r_f [$0^0/90^0/45^0/-45^0$]s (A)	8	1	6	1	0	90	45	-45	90.69	0	0	0	2071	400
t, r_f [$45^0/0^0/90^0/-45^0$]s (B)	1	8	7	1	45	0	90	-45	84.85	90.69	0	0	2220	400
t, r_f and θ (C)	8	1	1	6	0	32	-6	-35	90.51	0	0	0	2070	400

Table 12. Optimal design results of the laminated composite beams (fixed–pinned) for model 3

Design variable	Thickness (mm)	Fibre orientation (^{0})	Fiber volume fraction (%)	Weight (kg)	Frequency (Hz^2)

	t_1	t_2	t_3	t_4	θ_1	θ_2	θ_3	θ_4	$r_f^{(1)}$	$r_f^{(2)}$	$r_f^{(3)}$	$r_f^{(4)}$		
t, r_f $[0^0/90^0/45^0/-45^0]$s (A)	6	1	1	1	0	90	45	-45	89.02	0	0	0	1227	2500
t, r_f $[45^0/0^0/90^0/-45^0]$s (B)	1	4	1	5	45	0	90	-45	1.3	86.45	0	0	1349	2500
t, r_f and θ (C)	5	1	1	2	0	-1	-15	26	90.69	12.65	0	0	1194	2500

Table 13. Optimal design results of the laminated composite beams (pinned- pinned) for model 3

Design variable	Thickness (mm)				Fibre orientation (^{0})				Fiber volume fraction (%)				Weight (kg)	Frequency (Hz^2)
	t_1	t_2	t_3	t_4	θ_1	θ_2	θ_3	θ_4	$r_f^{(1)}$	$r_f^{(2)}$	$r_f^{(3)}$	$r_f^{(4)}$		
t, r_f $[0^0/90^0/45^0/-45^0]$s (A)	3	1	1	1	0	90	45	-45	80.86	0	0	0	762	400
t, r_f $[45^0/0^0/90^0/-45^0]$s (B)	1	2	3	1	45	0	90	-45	87.89	90.35	0	0	882	400
t, r_f and θ (C)	3	1	1	1	0	5	42	37	79.42	0	0	0	749	400

6. Conclusion

The paper deals with the multi-objective optimization problem for laminated composite beam structures. The objective functions are to minimum the weight of the whole laminated composite beam and maximize the natural frequency. The design variables include fiber volume fractions, thickness and fiber orientation angles of layers, in which the fiber volume fractions are taken as continuous design variables with the constraint on manufacturing process while the thickness and fiber orientation angles are discrete variables. The beam structure is subject to the constraint in the natural frequency which must be greater than or equal to a predetermined value. Three models with different combination of variables are investigated: (1) model 1 considers only one fiber volume fractions of layers as design variable; (2) model 2 considers both fiber volume fractions and thickness of layers and (3) model 3 considers all three design variables including thickness, fiber volume fractions and fiber orientation angles of layers. Then, the NSGA-II algorithm is employed to solve the multi-objective optimization problems.

Three numerical examples on a rectangle laminated composite beam structure with four different boundary conditions are performed. The obtained Pareto-optimal solutions are presented and discussed. From the numerical results, it can be seen that the optimal results of model 2 and model 3 outperform those of model 1. This is because of the presence of the design variable "thickness of the layers" in the models 2 and 3. In addition, the numerical results also show the useful effect of the third design variable "fiber orientation angles of layers" in the model 3 compared to the model 2. The results show that model 3 yields improved optimal solutions compared to those of model 2.

Acknowledgements

This research is funded by Vietnam National Foundation for Science and Technology Development (NAFOSTED) under grant number 107.99-2014.11.

References

[1] Ghashochi Bargh H, Sadr MH. Stacking sequence optimization of composite plates for maximum fundamental frequency using particle swarm optimization algorithm. Meccanica 2012;47:719–30. doi:10.1007/s11012-011-9482-5.

[2] Narita Y. Layerwise optimization for the maximum fundamental frequency of laminated composite plates. J Sound Vib 2003;263:1005–16. doi:http://dx.doi.org/10.1016/S0022-460X(03)00270-0.

[3] Apalak ZG, Apalak MK, Ekici R, Yildirim M. Layer optimization for maximum fundamental frequency of rigid point-supported laminated composite plates. Polym Compos 2011;32:1988–2000. doi:10.1002/pc.21230.

[4] Apalak MK, Karaboga D, Akay B. The Artificial Bee Colony algorithm in layer optimization for the maximum fundamental frequency of symmetrical laminated composite plates. Eng Optim 2014;46:420–37. doi:10.1080/0305215X.2013.776551.

[5] Sadr MH, Ghashochi Bargh H. Optimization of laminated composite plates for maximum fundamental frequency using Elitist-Genetic algorithm and finite strip method. J Glob Optim 2012;54:707–28. doi:10.1007/s10898-011-9787-x.

[6] Topal U. Frequency optimization of laminated composite plates with different intermediate line supports. Sci Eng Compos Mater 2012;19:295. doi:10.1515/secm-2012-0004.

[7] Hwang S-F, Hsu Y-C, Chen Y. A genetic algorithm for the optimization of fiber angles in composite laminates. J Mech Sci Technol 2014;28:3163–9. doi:10.1007/s12206-014-0725-y.

[8] Aymerich F, Serra M. Optimization of laminate stacking sequence for maximum buckling load using the ant colony optimization (ACO) metaheuristic. Compos Part A Appl Sci Manuf 2008;39:262–72. doi:10.1016/j.compositesa.2007.10.011.

[9] Jing Z, Fan X, Sun Q. Stacking sequence optimization of composite laminates for maximum buckling load using permutation search algorithm. Compos Struct 2015;121:225–36. doi:http://dx.doi.org/10.1016/j.compstruct.2014.10.031.

[10] Ho-Huu V, Do-Thi TD, Dang-Trung H, Vo-Duy T, Nguyen-Thoi T. Optimization of laminated composite plates for maximizing buckling load using improved differential evolution and smoothed finite element method. Compos Struct 2016;146:132–47. doi:10.1016/j.compstruct.2016.03.016.

[11] Hajmohammad MH, Salari M, Hashemi S a., Esfe MH. Optimization of stacking sequence of composite laminates for optimizing buckling load by neural network and genetic algorithm. Indian J Sci Technol 2013;6:5070–7.

doi:10.17485/IJST/2013/V6I8/36346.
[12] Adali S, Richter A, Verijenko VE, Summers EB. Optimal design of hybrid laminates with discrete ply angles for maximum buckling load and minimum cost. Compos Struct 1995;32:409–15. doi:10.1016/0263-8223(95)00067-4.
[13] Narita Y, Turvey GJ. Maximizing the buckling loads of symmetrically laminated composite rectangular plates using a layerwise optimization approach. Proc Inst Mech Eng Part C J Mech Eng Sci 2004;218:681–91. doi:10.1243/0954406041319554.
[14] Le-Anh L, Nguyen-Thoi T, Ho-Huu V, Dang-Trung H, Bui-Xuan T. Static and frequency optimization of folded laminated composite plates using an adjusted Differential Evolution algorithm and a smoothed triangular plate element. Compos Struct 2015;127:382–94. doi:10.1016/j.compstruct.2015.02.069.
[15] Ghasemi H, Kerfriden P, Bordas SPA, Muthu J, Zi G, Rabczuk T. Interfacial shear stress optimization in sandwich beams with polymeric core using non-uniform distribution of reinforcing ingredients. Compos Struct 2015;120:221–30. doi:http://dx.doi.org/10.1016/j.compstruct.2014.10.005.
[16] Ghasemi H, Brighenti R, Zhuang X, Muthu J, Rabczuk T. Optimal fiber content and distribution in fiber-reinforced solids using a reliability and NURBS based sequential optimization approach. Struct Multidiscip Optim 2015;51:99–112. doi:10.1007/s00158-014-1114-y.
[17] Ghasemi H, Brighenti R, Zhuang X, Muthu J, Rabczuk T. Optimization of fiber distribution in fiber reinforced composite by using NURBS functions. Comput Mater Sci 2014;83:463–73. doi:http://dx.doi.org/10.1016/j.commatsci.2013.11.032.
[18] Cho H-K. Design optimization of laminated composite plates with static and dynamic considerations in hygrothermal environments. Int J Precis Eng Manuf 2013;14:1387–94. doi:10.1007/s12541-013-0187-7.
[19] Liu Q. Exact sensitivity analysis of stresses and lightweight design of Timoshenko composite beams. Compos Struct 2016;143:272–86. doi:http://dx.doi.org/10.1016/j.compstruct.2016.02.028.
[20] Fan H-T, Wang H, Chen X-H. An optimization method for composite structures with ply-drops. Compos Struct 2016;136:650–61. doi:http://dx.doi.org/10.1016/j.compstruct.2015.11.003.
[21] Ghasemi H, Park HS, Rabczuk T. A level-set based IGA formulation for topology optimization of flexoelectric materials. Comput Methods Appl Mech Eng 2017;313:239–58. doi:http://dx.doi.org/10.1016/j.cma.2016.09.029.
[22] Nanthakumar SS, Valizadeh N, Park HS, Rabczuk T. Surface effects on shape and topology optimization of nanostructures. Comput Mech 2015;56:97–112. doi:10.1007/s00466-015-1159-9.
[23] Liu Q. Analytical sensitivity analysis of eigenvalues and lightweight design of composite laminated beams. Compos Struct 2015;134:918–26. doi:10.1016/j.compstruct.2015.09.002.
[24] Liu Q, Paavola J. Lightweight design of composite laminated structures with frequency constraint. Compos Struct 2015. doi:10.1016/j.compstruct.2015.08.116.
[25] Vo-Duy T, Ho-Huu V, Do-Thi TD, Dang-Trung H, Nguyen-Thoi T. A global numerical approach for lightweight design optimization of laminated composite plates subjected to frequency constraints. Compos Struct 2017;159:646–55. doi:10.1016/j.compstruct.2016.09.059.
[26] Pelletier JL, Vel SS. Multi-objective optimization of fiber reinforced composite laminates for strength, stiffness and minimal mass. Comput Struct 2006;84:2065–80. doi:http://dx.doi.org/10.1016/j.compstruc.2006.06.001.
[27] Lee DS, Morillo C, Bugeda G, Oller S, Onate E. Multilayered composite structure

design optimisation using distributed/parallel multi-objective evolutionary algorithms. Compos Struct 2012;94:1087–96. doi:http://dx.doi.org/10.1016/j.compstruct.2011.10.009.
[28] Vosoughi AR, Nikoo MR. Maximum fundamental frequency and thermal buckling temperature of laminated composite plates by a new hybrid multi-objective optimization technique. Thin-Walled Struct 2015;95:408–15. doi:http://dx.doi.org/10.1016/j.tws.2015.07.014.
[29] Honda S, Igarashi T, Narita Y. Multi-objective optimization of curvilinear fiber shapes for laminated composite plates by using NSGA-II. Compos Part B Eng 2013;45:1071–8. doi:http://dx.doi.org/10.1016/j.compositesb.2012.07.056.
[30] Deb K, Pratap A, Agarwal S, Meyarivan T. A fast and elitist multiobjective genetic algorithm: NSGA-II. IEEE Trans Evol Comput 2002;6:182–97. doi:10.1109/4235.996017.
[31] Robert M. Jones. Mechanics Of Composite Materials. 2 edition. CRC Press; 1998.
[32] Altenbach H, Altenbach J, Kissing W. Mechanics of Composite Structural Elements. 1st ed. Berlin, Heidelberg: Springer Berlin Heidelberg; 2004. doi:10.1007/978-3-662-08589-9.
[33] Marler RT, Arora JS. Survey of multi-objective optimization methods for engineering. Struct Multidiscip Optim 2004;26:369–95. doi:10.1007/s00158-003-0368-6.
[34] Zitzler E, Laumanns M, Thiele L. SPEA2: Improving the strength Pareto evolutionary algorithm. Eurogen, vol. 3242, 2001, p. 95–100.
[35] Zhang Q, Li H. MOEA/D: A Multiobjective Evolutionary Algorithm Based on Decomposition. IEEE Trans Evol Comput 2007;11:712–31. doi:10.1109/TEVC.2007.892759.
[36] Srinivas N, Deb K. Muiltiobjective Optimization Using Nondominated Sorting in Genetic Algorithms. Evol Comput 1994;2:221–48. doi:10.1162/evco.1994.2.3.221.
[37] Liu GR, Chen SC. Flaw detection in sandwich plates based on time-harmonic response using genetic algorithm. Comput Methods Appl Mech Eng 2001;190:5505–14. doi:http://dx.doi.org/10.1016/S0045-7825(01)00173-6.
[38] Zheng H, Cai C, Pau GSH, Liu GR. Minimizing vibration response of cylindrical shells through layout optimization of passive constrained layer damping treatments. J Sound Vib 2005;279:739–56. doi:http://dx.doi.org/10.1016/j.jsv.2003.11.020.
[39] Liu GR, Ma HJ, Wang YC. Material characterization of composite laminates using dynamic response and real parameter-coded microgenetic algorithm. Eng Comput 2005;20:295–308. doi:10.1007/s00366-004-0298-y.
[40] Xu YG, Liu GR, Wu ZP. Damage Detection for Composite Plates Using Lamb Waves and Projection Genetic Algorithm. AIAA J 2002;40:1860–6. doi:10.2514/2.1865.
[41] Goldberg DE. Genetic Algorithms in Search, Optimization, and Machine Learning. Reading, MA: Addison-Wesley; 1989.
[42] Dhanalakshmi S, Kannan S, Mahadevan K, Baskar S. Application of modified NSGA-II algorithm to Combined Economic and Emission Dispatch problem. Int J Electr Power Energy Syst 2011;33:992–1002. doi:http://dx.doi.org/10.1016/j.ijepes.2011.01.014.
[43] Kannan S, Baskar S, McCalley JD, Murugan P. Application of NSGA-II Algorithm to Generation Expansion Planning. IEEE Trans Power Syst 2009;24:454–61. doi:10.1109/TPWRS.2008.2004737.
[44] Martínez-Vargas A, Domínguez-Guerrero J, Andrade ÁG, Sepúlveda R, Montiel-Ross O. Application of NSGA-II algorithm to the spectrum assignment problem in spectrum sharing networks. Appl Soft Comput 2016;39:188–98. doi:http://dx.doi.org/10.1016/j.asoc.2015.11.010.

[45] Soyel H, Tekguc U, Demirel H. Application of NSGA-II to feature selection for facial expression recognition. Comput Electr Eng 2011;37:1232–40. doi:http://dx.doi.org/10.1016/j.compeleceng.2011.01.010.
[46] Yu X, Liong S-Y, Atiquzzaman M. Alternative Decision Making in Water Distribution Network with NSGA-II 2006. doi:10.1061/(ASCE)0733-9496(2006)132:2(122).